Received: 29 March 2019 | Accepted: 2 May 2019

DOI: 10.1002/pamm.201900032

# A bottom-up continuum approach of crystal plasticity for the analysis of fcc microwires under torsion

**Kolja Zoller**[1,*] and **Katrin Schulz**[1,**]

[1] Institute for Applied Materials - Computational Materials Science (IAM-CMS), Karlsruhe Institute of Technology, Kaiserstr.12, 76131 Karlsruhe, Germany

The microstructural evolution of face-centered cubic microwires is studied using a physical motivated, homogenized continuum model of crystal plasticity. The dislocation configuration in the three-dimensional space is thereby described via a Continuum Dislocation Dynamics (CDD) theory including a dislocation source term. The resulting spatial distribution of dislocation densities and strain components are shown for a relaxation problem with torsional loading.



## 1 Introduction

Microwires under torsion show a pronounced size effect [1], whereby the consideration of single crystal allows to study the influence of strain gradients independent from grain sizes. Describing dislocation densitiy as a homogenized ensemble of dislocation lines, the CDD theory [2] is suitable for a physical consideration of such problem providing the benefits of a continuum formulation. An extension including a dislocation density production term for bending is formulated in [3]. The connection between pile-ups and size effects is discussed in [4].

## 2 Dislocation density based continuum model

The considered model describes the elasto-plastic deformation behavior of face-centered cubic single crystal metals, whereby the plasticity solely results from the evolution of the dislocation microstructure characterized by CDD densities. Operating on the mesoscopic scale, the model can be divided into two coupled problems using the same length scale: The elastic problem calculating the stress field $\boldsymbol{\sigma}$ for a given plastic state and the dislocation problem describing the dislocation evolution for a given stress field resulting in plasticity via the plastic slip $\gamma_s$ on all twelve slip systems $S = 12$. Each slip systems $s$ is characterized by its plane normal $\boldsymbol{m}_s$ and the Burger's vector $\boldsymbol{b}_s = b_s \boldsymbol{d}_s$ with the length $b_s$ and the slip direction $d_s$. The governing equations of both problems can be found in Tab. 1. Regarding the boundaries, it has to be remarked, that the dislocations can leave the continuum at the surfaces unhindered. The considered degrees of freedom are three nodal displacements plus four nodal dislocation density based quantities per slip system.

The curvature production term $\dot{q}_s^{prod}$ enables the model to increase the number of dislocation loops in the system. The production term is activated if the local stress exceeds a critical value and accounts for a relaxation of the local stress to its critical state. The macroscopic ideal plastic material behavior functions thereby as a upper limit for the global production rate.

**Table 1:** Set of governing equations in the three-dimensional space

| Elastic problem | | Dislocation problem | |
|---|---|---|---|
| Decomposed distorsion tensor | $\mathrm{D}\boldsymbol{u} = \boldsymbol{\beta}^{\mathrm{el}} + \boldsymbol{\beta}^{\mathrm{pl}}$ | Orowan equation | $\dot{\gamma}_s = v_s b_s \rho_s$ |
| Plastic distorsion | $\boldsymbol{\beta}^{\mathrm{pl}} = \sum_{s=1}^{S} \gamma_s \boldsymbol{M}_s$ | Velocity law | $v_s = \frac{b_s}{B} \operatorname{sgn}(\tau_s^{\mathrm{eff}}) \max\left\{0, \lvert\tau_s^{\mathrm{eff}}\rvert - \tau_s^{\mathrm{y}}\right\}$ |
| Schmid tensor | $\boldsymbol{M}_s = \boldsymbol{d}_s \otimes \boldsymbol{m}_s$ | Effective stress | $\tau_s^{\mathrm{eff}} = \boldsymbol{\sigma} \cdot \boldsymbol{M}_s - \tau_s^{\mathrm{b}}$ |
| Infinitesimal total strain | $\boldsymbol{\varepsilon} = \operatorname{sym} D\boldsymbol{u}$ | Backstress | $\tau_s^{\mathrm{b}} = \frac{D\mu b_s}{\rho_s} \nabla \cdot \boldsymbol{\kappa}_s^{\perp}$ , $\boldsymbol{\kappa}_s^{\perp} = \boldsymbol{\kappa}_s \times \boldsymbol{m}_s$ |
| Stress-strain relation | $\boldsymbol{\sigma} = \mathbb{C}[\boldsymbol{\varepsilon} - \boldsymbol{\varepsilon}^{\mathrm{pl}}]$ | Yield stress | $\tau_s^{\mathrm{y}}(\boldsymbol{\rho}) = a\mu b_s \sqrt{\sum_n \rho_n}$ |
| Macroscopic balance equation | $-\operatorname{div} \boldsymbol{\sigma} = \boldsymbol{f}_{\mathcal{B}}$ | Dislocation density | $\dot{\rho}_s = -\nabla \cdot \left(v_s \boldsymbol{\kappa}_s^{\perp}\right) + v_s q_s$ |
| Dirichlet boundary conditions | $\boldsymbol{u} = \boldsymbol{u}_{\mathrm{D}}$ | GND density | $\dot{\boldsymbol{\kappa}}_s = \nabla \times (\rho_s v_s \boldsymbol{m}_s)$ |
| Neumann boundary conditions | $\boldsymbol{\sigma}\boldsymbol{n} = \boldsymbol{t}_{\mathrm{N}}$ | Curvature density | $\dot{q}_s = -v_s \nabla \cdot \left(\frac{q_s}{\rho_s} \boldsymbol{\kappa}_s^{\perp}\right) + \dot{q}_s^{prod}$ |
| | | | $-\frac{1}{2}\left(\left(\rho_s + \lvert\boldsymbol{\kappa}_s\rvert\right) \frac{\boldsymbol{\kappa}_s}{\lvert\boldsymbol{\kappa}_s\rvert} \otimes \frac{\boldsymbol{\kappa}_s}{\lvert\boldsymbol{\kappa}_s\rvert} + \left(\rho_s - \lvert\boldsymbol{\kappa}_s\rvert\right) \frac{\boldsymbol{\kappa}_s^{\perp}}{\lvert\boldsymbol{\kappa}_s^{\perp}\rvert} \otimes \frac{\boldsymbol{\kappa}_s^{\perp}}{\lvert\boldsymbol{\kappa}_s^{\perp}\rvert}\right) \cdot \nabla^2 v_s$ |
| | | Boundary condition | $v_s\Big(\lvert\boldsymbol{n} \times \boldsymbol{m}_s\rvert \rho_s + (\boldsymbol{n} \times \boldsymbol{m}_s) \cdot \boldsymbol{\kappa}_s\Big) = 0$ |

* Corresponding author: e-mail kolja.zoller@kit.edu, phone +49 721 608-45869, fax +49 721 608-44364
** e-mail katrin.schulz@kit.edu

## 3 Relaxation of micro-torsion

The used system configuration is shown in Fig. 1. A microwire with an aspect ratio of one to two is examined. The bottom is fixed and the top is subjected to a twist deformation. The surfaces on the side are traction-free. We consider an instantaneous loading with an subsequent dislocation relaxation. The resulting stress field consists mainly of two shear components with a linear distribution. Therefore, the center is stress-free and the highest stress occurs at the surface. The chosen material parameter in Tab. 2 are based on aluminium with a [0 1 0] crystal orientation. Elastic isotropy is assumed.

The initial condition is dislocation free and the critical stress for the source activation is adapted in such a way, that the stresses at the surface reach the double of the critical value in the initial step. For the elastic problem a standard FEM solver with linear ansatz functions is used. The flux-based dislocation transport equations considering dislocation mean-field stresses are solved by a Runge-Kutta discontinuous Galerkin scheme with upwind flux, an implicit midpoint rule for the evolution equations and quadratic ansatz functions. Both solvers operate on the same mesh consisting of about 170 000 tetragonal elements. The spatial distribution over the radius of the resulting microstructure is characterized by Fig. 2 and Fig. 3.

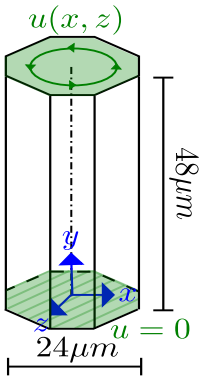


**Fig. 1:** Geometry

**Table 2:** Material parameter

| | | |
|---|---|---|
| $\mu$ = | 27 | GPa |
| $\nu$ = | 0.347 | |
| $b$ = | 0.286 | μm |
| $B$ = | $10^{-4}$ | ns GPa |
| $D$ = | 0.255 | $\mu m^{-3}$ |
| $a$ = | 0.3 | $\mu m^{-2}$ |

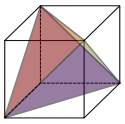

Crystal Orientation: [0 1 0]

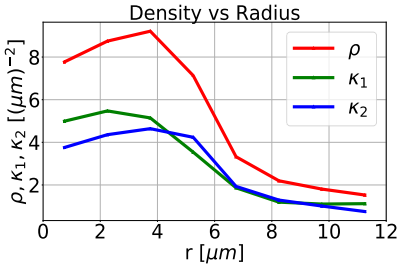


**Fig. 2:** Resulting spatial distribution over the radius $r = \sqrt{x^2 + z^2}$ of the total dislocation density $\rho$ as well as screw part $\kappa_1$ and edge part $\kappa_2$ of the GND density measured in the middle of the microwire.

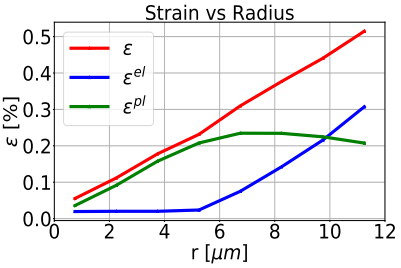


**Fig. 3:** Resulting spatial distribution over the radius $r = \sqrt{x^2 + z^2}$ of the total strain $\varepsilon$ and its elastic part $\varepsilon^{el}$ and plastic part $\varepsilon^{pl}$ measured in the middle of the microwire.

The expanding dislocation loops produced near the surface in the initial step are leaving the continuum at the surfaces and moving accordingly to the stress field towards the center forming a pile-up. Accordingly, the piled-up total dislocation density consists mainly of geometrically necessary dislocation (GND) density. Due to the orientation of the slip systems and loading case, the screw and edge part of the GNDs are nearly of the same amount.

The total strain has a linear profile over the radius. The resulting plastic strain is nearly constant near the surface and decreases from a breaking point linear towards the center in the same manner as the total strain. The position of the break point correlates with the change in the dislocation density. The elastic strain and therefore the shear stress is almost zero near the center and increase linear from the break point towards the surface with the same gradient as the total strain.

## 4 Discussion

With the critical thickness theory (CTT) there are analytical studies on this topic [5]. When the strain reaches a critical state, the area under the elastic strain curve remains constant in the following. The qualitative distribution found by CTT is identical to the simulation results in this contribution. For the given load even the quantitative distribution is similar except for a constant higher dislocation production by a factor of one third. This is due to the three-dimensional consideration with an increasing influence over the radius since each element has the same weight but the area increase with the radius.

One important point is that we wouldn't expect such a qualitative behavior for a classical continuum approach. The flow terms of the CDD formulation enable the dislocation produced near the surface to move into the center and therefore plastify even the material with a local stress smaller than the critical value.

**Acknowledgements** The financial support for this work in the context of the DFG research group FOR1650 'Dislocation based Plasticity' as well as the support by the European Social Fund and the state Baden-Wuerttemberg is gratefully acknowledged. This work was performed on the computational resource ForHLR II funded by the Ministry of Science, Research and the Arts Baden-Württemberg and DFG.

## References

[1] N. A. Fleck, G. M. Muller, M. F. Ashby, and J. W. Hutchinson, Acta metall. mater. **42(2)**, 475–487 (1994).
[2] T. Hochrainer, S. Sandfeld, M. Zaiser, and P. Gumbsch, J. Mech. Phys. Solids **63**, 167–178 (2014).
[3] S. Schmitt, M. Stricker, P. Gumbsch, and K. Schulz, Acta Materialia **164**, 663–672 (2019).
[4] K. Schulz, M. Sudmanns, and P. Gumbsch, Modelling Simul. Mater. Sci. Eng. **25(6)**, 064003 (2017).
[5] D. Liu, X. Zhang, Y. Li and D. J. Dunstan, Acta Materialia **150**, 213-223 (2018).

 